Paleobiology, 27(4), 2001, pp. 735–750

Estimating body mass from silhouettes: testing the assumption of elliptical body cross-sections

Ryosuke Motani

Abstract.—In computational studies of the body mass and surface area of vertebrates, it is customary to assume that body cross-sections are approximately elliptical. However, a review of actual vertebrate cross-sections establishes that this assumption is not usually met. A new cross-sectional model using superellipses is therefore introduced, together with a scheme that allows estimates to be given with ranges. Tests of the new method, using geometrical shapes, miniature vertebrate models, and actual animals, show that the method has a high accuracy in body mass estimation. A new computer program to perform the computation is introduced. The application of the method to some Mesozoic marine reptiles suggests that the tuna-shaped ichthyosaur *Stenopterygius* probably had body masses comparable to those of average cetaceans of the same body length.

Ryosuke Motani. Department of Palaeobiology, Royal Ontario Museum, 100 Queen's Park, Toronto, Ontario M5S 2C6, Canada. E-mail: ryo.motani@utoronto.ca

Accepted: 17 May 2001

Introduction

Body mass and surface area are among the most fundamental characteristics of animals. These values are essential elements of physiology and biomechanics (e.g., Schmidt-Nielsen 1997; Alexander 1998), and therefore it is important for biologists to make accurate estimates. For example, in energetic studies of dolphins, a 10% error in surface area estimate would produce about a 9% error in drag coefficient, whereas 10% overestimation of body mass would result in about a 9% error in calculating mass-specific metabolic rates from metabolic rate measurements.

Despite such importance, body mass estimation involves errors not only for extinct animals, but also for some extant animals whose body mass is difficult to measure directly (e.g., whales). For example, a series of studies conducted by the Whale Research Institute of Tokyo around 1950 (e.g., Nishiwaki and Hayashi 1950; Nishiwaki and Oye 1951) measured large whales by dividing the great carcasses into small blocks. Although they tried to capture the blood along with bone- and meat-residues resulting from the sawing of the carcasses, some blood escaped, leading to underestimation of body mass (but the proportion of error was probably small, as discussed later). Body surface area estimation is problematic for virtually all animals, both extant and extinct. Therefore, it is a shared interest of paleontologists and neontologists to establish methods to estimate body mass and surface area without direct measurement, and to quantify the error levels of such methods.

Both neontologists and paleontologists have attempted body mass estimation in the past. There is a common feature in these studies: they first calculate the volume of a given animal and then convert it to body mass by multiplying it by the density of water. Henderson (1999) recently reviewed such studies concerning extinct vertebrates, so it is not repeated here. These studies are divided into two categories: those that use actual scaled models (Gregory 1905; Colbert 1962; Alexander 1985), and those that use computerized mathematical models (Henderson 1999; this study). Mathematical models have also been used in neontological studies to estimate body mass and surface area of whales. For example, Bose and Lien (1989) calculated the body mass and surface area of a 14.5-m fin whale from girth (or half-girth) measurements taken at a constant interval along the body axis. They assumed elliptical cross-sections of varying eccentricity for the body to facilitate volume computation. Also, Fish (1993, 1998) estimated the surface area of four odontocete species from photographs, assuming elliptical body cross-sections.

 0094-8373/01/2704-0009/$1.00

TABLE 1. Fork length and fluke dimensions of eight cetacean species. Abbreviations: FL = fork length; Aflat = flat area of the fluke (see text); S = surface area of the fluke; V = volume of the fluke. Calculated from data presented by Bose et al. (1990). E-02 = 10^{-2}, etc.

Species		FL (m)	Aflat (m^2)	S (m^2)	V (m^3)
Harbor porpoise	*Phocoena phocoena*	1.8	1.78E-02	3.96E-02	2.05E-04
		1.47	3.87E-02	8.74E-02	7.98E-04
White-sided dolphin	*Lagenorhynchus acutus*	1.42	3.23E-02	7.34E-02	6.56E-04
White-beaked dolphin	*L. albirostris*	2.22	7.77E-02	1.71E-01	1.61E-03
Common dolphin	*Delphinus delphis*	2.5	5.30E-02	1.71E-01	7.50E-04
White whale	*Delphinapterus leucas*	3.79	2.47E-01	5.45E-01	8.80E-03
Sowerby's beaked whale	*Mesoplodon physalus*	4.64	2.32E-01	5.25E-01	7.05E-03
Minke whale	*Balaenoptera acutorostrata*	6.14	4.95E-01	1.11	2.04E-02
Fin whale	*B. physalus*	14.5	1.82	4.02	1.65E-01

Henderson's (1999) study represents the most elaborate mathematical modeling of body mass and surface area to date. He outlined a method to construct three-dimensional computer models of vertebrates on the basis of their orthogonal silhouettes, and he used a scientific visualization software package to calculate the volume and surface area of the models. The coordinates of selected points along the silhouette outline were obtained with a digitizing tablet, and then imported to the software. Like Bose and Lien (1989), he assumed elliptical body cross-sections to generate three-dimensional models from two-dimensional silhouettes. Although this study was a remarkable technical refinement, its accuracy was compromised by (1) errors introduced during manual operation of digitizing tablets (Henderson 1999: p. 105) and (2) the slice count of 32 or fewer for the entire body, which may be sufficient for such simple shapes as ellipsoids (Henderson 1999: p. 96), but not for more complicated shapes of vertebrates that usually contain multiple inflection points.

All mathematical models thus far developed share the important simplifying assumption that body cross-sections are elliptical. Despite its popularity, this assumption has never been rigorously tested. Bose et al. (1990) tested the method of Bose and Lien (1989) by applying it to smaller whales with known body masses. They found that the method underestimated the true body mass by a factor of up to 31.7% (based on Bose et al. 1990: Table 1). This study indicates that the assumption of elliptical body cross-sections is often not met in nature.

The purpose of the present paper is threefold. First, I test the assumption of elliptical body cross-sections and propose an alternative model. Second, I describe a method to calculate body mass and surface area from orthogonal silhouettes of vertebrates. The method, empowered by the new cross-sectional model, is more accurate in many cases and simpler to perform than that presented by Henderson (1999). An earlier version of the method was used by Motani et al. (1999). Third, I test the method with a wide range of data, and apply it to some Mesozoic marine reptiles.

Body and Limb Cross-Sections in Vertebrates

The cross-sectional shape changes extensively along the axis of a given vertebrate, which makes it difficult to construct a uniform mathematical model. The cross-sections are usually not truly elliptical, although there are exceptions. When cross-sections of vertebrate body parts are compared with ellipses that share their heights and widths (Fig. 1), the following is commonly observed:

Trunk (Fig. 1A–K).—In the presacral region, the elliptical approximation almost always underestimates the true area of cross-sections in tetrapods, except in the lumbar area of some species (Fig. 1B,K). The perimeters of the true cross-sections are always longer than those of the ellipses, even when the area is overestimated by ellipses (Fig. 1B,K). These

indicate that the assumption of elliptical cross-sections leads to underestimation of both volume and surface area of the trunk region of tetrapods. In teleosts, ellipses tend to overestimate the actual cross-sectional areas (Fig. 1E), except in species with somewhat round bodies, such as tunas (Fig. 1C,D).

Tail (Fig. 1L–P).—In the caudal region of *Alligator sinensis*, the ellipses always overestimate the true cross-sectional areas (Fig. 1L–O), and the same is observed for the Atlantic mackerel (*Scomber scombrus*; Fig. 1P), except in the peduncular area where the cross-sections are well approximated by ellipses. The true perimeter is underestimated by the ellipses in all vertebrates examined. The tails are much lighter than the presacral areas in most tetrapods, so the true volume is probably underestimated by the assumption of elliptical cross-sections when the presacral and caudal regions are combined. In most teleosts, the use of ellipses probably leads to overestimation of the true volume, except possibly in tunas and similarly shaped forms.

Limb (Fig. 1Q–Z).—Vertebrate limbs differ from their main bodies in that the variation of cross-sectional shape is much more pronounced than in the latter. The ellipses underestimate the perimeter, whereas the cross-sectional area may or may not be underestimated. Therefore, the surface area of a vertebrate limb is always underestimated by the assumption of elliptical cross-sections, whereas its volume may or may not be. On average, it is probably reasonable to assume elliptical cross-sections for limb volume estimation when no actual cross-section is available.

Superellipse.—The above observations are far from exhaustive, but it is at least evident that elliptical cross-sections compromise the quality of modeling of vertebrate bodies. The modeling accuracy may be improved by introducing other cross-sectional shapes, such as the superellipse. The superellipse is defined by the equation

$$|x/a|^k + |y/b|^k = 1 \qquad (1)$$

where a and b are the lengths of the major and minor semi-axes, and k is an exponential constant that determines the degree of "swelling" (Fig. 2A). The ellipse is a special case of the superellipse, with a k-value of 2.0. As the value of k increases from 2.0, the superellipse approaches the rectangle, whereas it approaches a rhomboid as k decreases toward 1.0 (Fig. 2A). At k-values of below 1.0, the superellipse approaches a cross shape, passing through the asteroid at a k-value of 2/3. The superellipse was invented by Piet Hein (Gardner 1965) and is used, along with its three-dimensional extension called the superellipsoid, or, more inclusively, superquadric, in computer modeling of three-dimensional shapes (e.g., Barr 1981; Pilu and Fisher 1995; Rosin and West 1995).

Superelliptical body cross-sections are also found in nature, including cross-sections of vertebrates (Fig. 2C–H). For example, the cross-section of the trunk of a kawakawa (*Euthynnus affinis*), figured by Dewar et al. (1994: Fig. 1A), is very closely approximated by a superellipse with a k-value of 2.5 (Fig. 2B). Many cross-sections through the bodies of vertebrates are not dorsoventrally symmetrical, the dorsal half having higher k-values than its ventral counterpart. A superellipse with a k-value of 2.5, for example, approximates a cross-section through the human thoracic region dorsally, whereas the k-value is about 2.0 ventrally (Figs. 1F, 2F–H).

It is best to examine the actual cross-sections when determining k-values for each slice of the body of a given vertebrate. Such a procedure is not possible for extinct animals, but this does not mean that one should assume elliptical cross-sections (i.e., $k = 2.0$). Assuming k-values to be constantly 2.0 for tetrapods is probably less reasonable than assuming a constant value of, say, 2.2. One way to proceed is to choose two k-values that most likely represent the upper and lower limits within a given animal, and then estimate body mass with a range using these values. Such k-values may be 2.5 (upper limit) and 2.0 (lower limit) in the cases examined above for tetrapods, but some cetaceans may have higher values (see below). For most teleosts, the values may be about 2.0 and 1.5, but they should probably be 2.5 and 2.0 for tunas and similarly shaped forms. In the future, it is desirable to examine as many extant animals as possible for the variation of k-values along the body. These data should

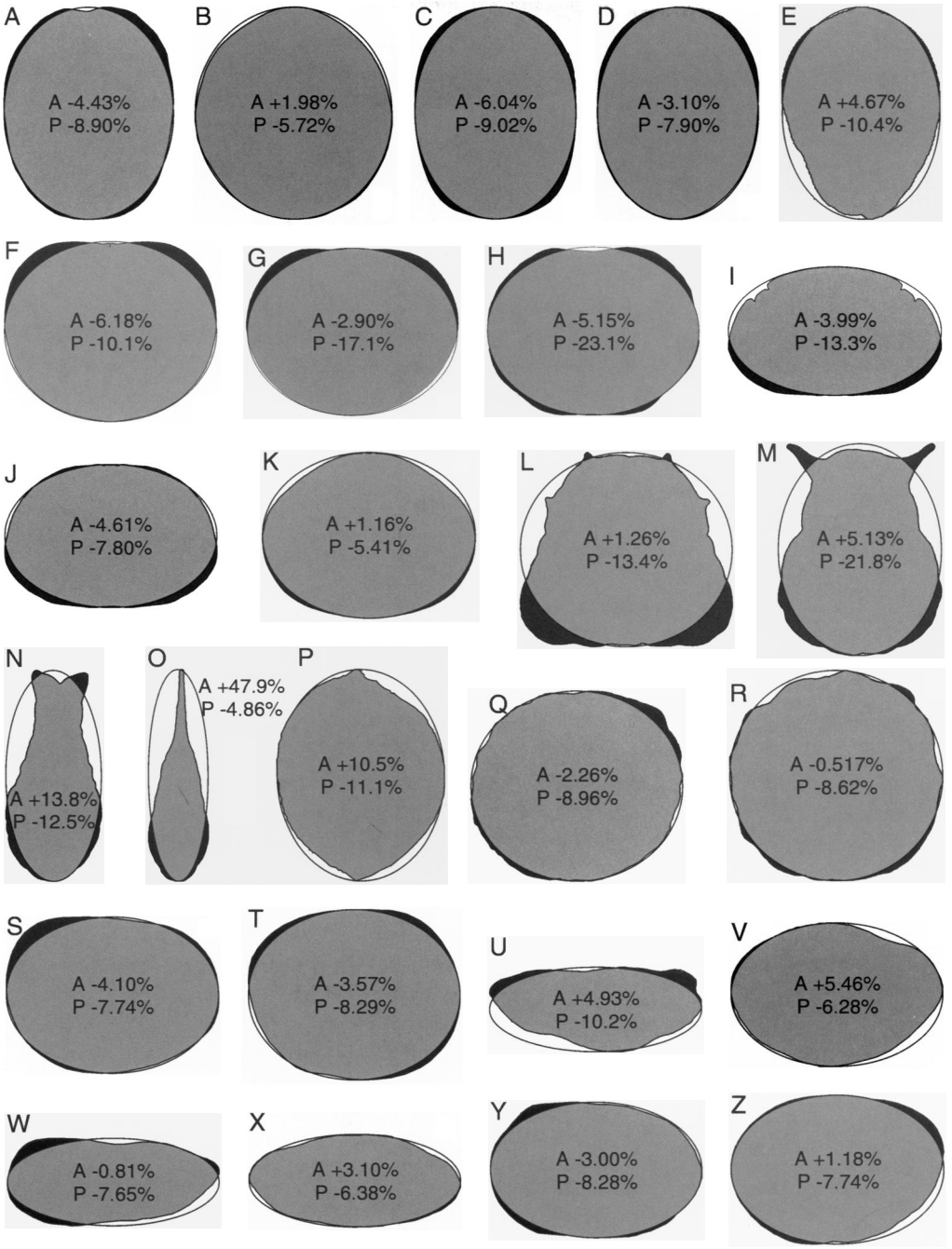

FIGURE 1. Cross-sections of the body and limbs of selected vertebrates, compared with ellipses that share their heights and widths. Gray areas are commonly shared by the actual cross-section and its elliptical model. Areas where cross-sections are larger than ellipses are painted black, whereas the area is left white if the ellipses are larger than the cross-sections. The numbers given represent how much the true area (A) and perimeter (P) are overestimated by elliptical models. For example, "A−4.43%" indicates that the actual cross-section is underestimated by the ellipse by 4.43%. A, Thoracic section of a rabbit; B, Lumbar section of a rabbit; C, Trunk section of a kawakawa (*Euthynnus affinis*); D, Trunk section of a yellowfin tuna (*Thunnus albacares*); E, Cloacal section of an Atlantic mackerel (*Scomber scombrus*); F, Cervical section of a human; G, Thoracic section of a human (at T11); H, Thoracic section of a human (at T12); I, Spiracular section of a dogfish (*Squalus acanthias*); J, Thoracic section of a Chinese alligator (*Alligator sinensis*); K, Lumbar section of the same; L, Anterior caudal section of the same; M, The same, but slightly posterior; N, Middle caudal section of a Chinese alligator; O, Posterior caudal section of the same;

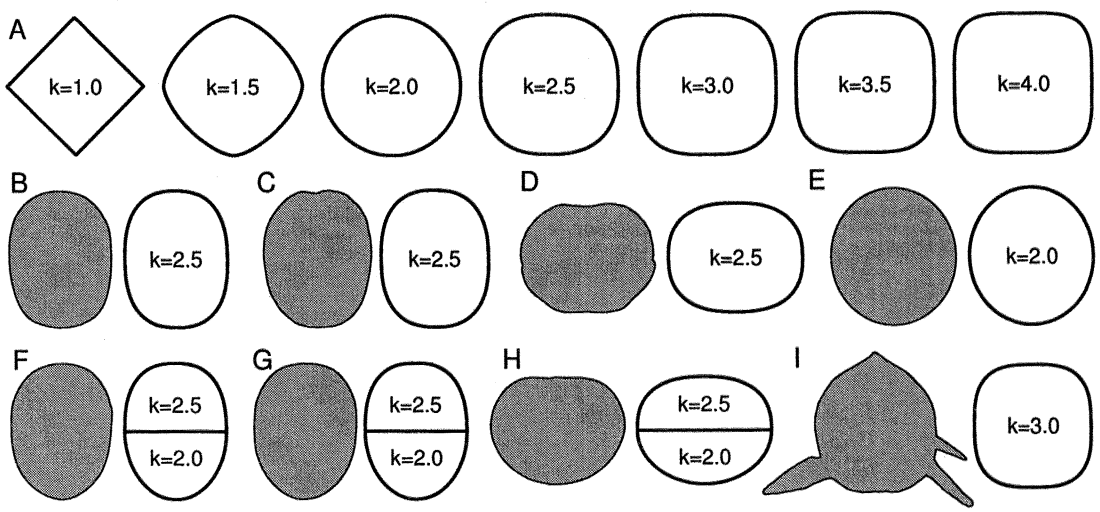

FIGURE 2. Superellipses, and their occurrences in vertebrate cross-sections. A, Examples of superelliptical shapes with varying exponent value (k) of equation (1); B, Trunk section of a kawakawa (*Euthynnus affinis*), compared with a superellipse; C, Thoracic section of a rabbit; D, Thoracic section of a human (at T12); E, Lumber section of a rabbit; F, Trunk section of a yellowfin tuna (*Thunnus albacares*); G, Trunk section of a bluefin tuna (*Thunnus thynnus*); H, Thoracic section of a human (at T11); I, Anterior view of a white whale (*Delphinapterus leucas*). B, F, and G based on Dewar et al. 1994. C and E based on Graigie 1966. D and H based on Mori et al. 1982. I based on Murayama and Kasamatsu 1996.

then be combined with analogies based on habitats and behavior, as well as phylogenetic brackets (Bryant and Russell 1992; Witmer 1995) when possible, to infer k-values in extinct vertebrates.

Methods

Data Preparation (Fig. 3).—The first step is to obtain orthogonal views of vertebrates (Fig. 3A). These are usually lateral and dorsal views for aquatic vertebrates with flippers, whereas anteroposterior views are also needed for terrestrial vertebrates in order to constrain limb shapes. Such protruding structure as limbs, fins, and flukes are then separated from the main body (Fig. 3B). In the present study, this process was done in a vector-based drawing program (CorelDraw 9) and used vector outlines of silhouettes traced from bitmap images using CorelTrace 9. After the separation, each view of each body part is saved in a separate bitmap file (each body part should have two bitmap files representing orthogonal views around its longitudinal axis to constrain three-dimensional shapes, except finlike elements). The dot counts of these images determine the sampling rate during the calculation that follows. For example, if the body is 1000 dots axially, it will be analyzed in 1000 slices. Scales are kept constant among views of a single body part (e.g., if the lateral view of the body is 1000 dots long, its dorsoventral view should also be 1000 dots long). Once the bitmap images are made, they are converted to coordinate data (Fig. 3C). This is easily achieved by free software packages, such as ImageTool and NIH Image.

Calculation (Fig. 4).—The calculation of volume and surface area is done in slices, with dots as the unit. The unit will later be converted to the International System (SI) according to the calibration factor of the original im-

←

P, Caudal section of an Atlantic mackerel; Q, Upper arm section of a Chinese alligator; R, Thigh section of the same; S, Upper arm section of a human; T, Thigh section of the same; U, Thigh section of a cat; V, Forearm section of the same; W, Upper arm section of a rabbit; X, Thigh section of the same; Y, Lower leg section of the same; Z, Lower leg section of a cat. A, B, and W–Y based on Graigie 1966; C and D based on Dewar et al. 1994; E and P based on personal data; F–H, S, and T based on Mori et al. 1982; I based on Walker and Homberger 1992; J–O, Q, and R based on Cong et al. 1998; U, V, and Z based on Gilbert 1968.

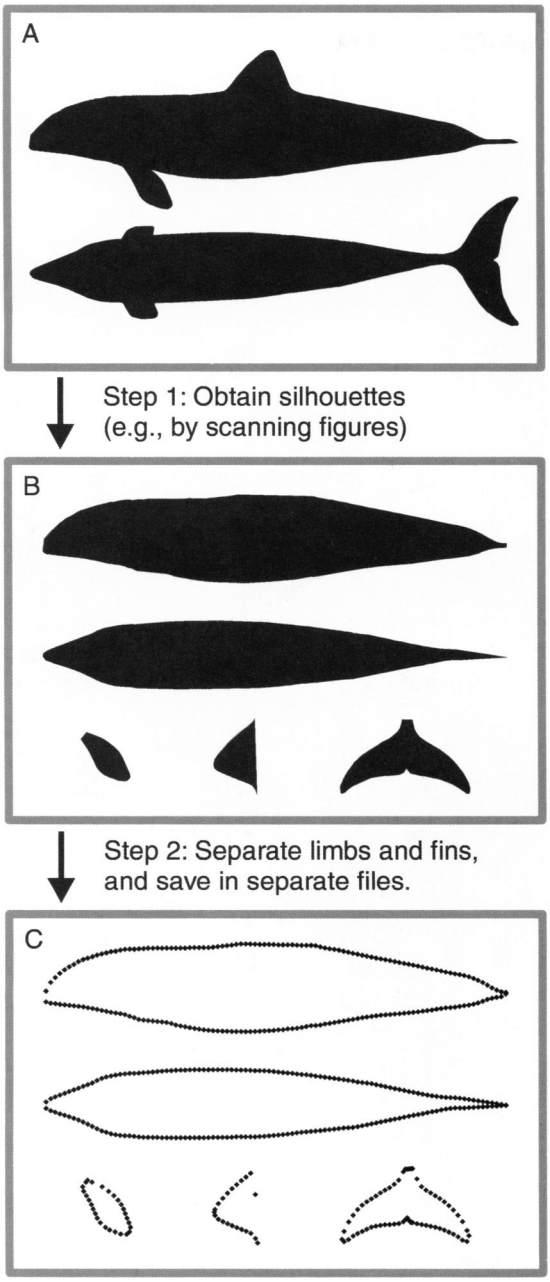

FIGURE 3. Outline of the data preparation for the present method. The coordinates of the body outline are directly obtained from bitmap images, without manual digitization.

ages. The width of each slice corresponds to one dot of the original bitmap image (Fig. 4C).

For the main body and limbs, the height and width of each three-dimensional slice are obtained by slicing two-dimensional views from orthogonal directions (e.g., lateral and dorsal views for the main body; Fig. 4A). A superellipse with the obtained width and height is constructed around the center of the slice (Fig. 4B). The exponent k of the superellipse is set to the most appropriate values when known from cross-sections. Otherwise, the upper and lower limits of k are set to compute the results with ranges, as discussed earlier. From the superellipses thus constructed, the volume and surface area of each slice is approximated as in Figure 4C. The volume of the i^{th} slice (V_i) is calculated as that of a superelliptical cone frustum, with the height of one dot. This is given as

$$V_i = (A_i + A_{i+1} + (A_iA_{i+1})^{0.5})/3$$

where A_i denotes the area of the i^{th} cross-section, which is calculated as the area of a superellipse. When two subaxes of a superellipse are equal and have a unit length, its area ($A_{SE\text{-}UNIT}$) is given as

$$A_{SE\text{-}UNIT}(k) = 4\int_0^1 (1 - x^k)^{1/k}\,dx$$

The more general equation for the area of a superellipse (A_{SE}) is given as

$$A_{SE}(k) = 4b\int_0^a [1 - (x/a)^k]^{1/k}\,dx$$

$$= 4ab\int_0^1 (1 - t^k)^{1/k}\,dt = abA_{SE\text{-}UNIT}(k)$$

Thus, the area of a superellipse as in equation (1) is $a \times b$ times that of a unit superellipse with the same exponent k.

The surface area of the i^{th} slice (S_i) is calculated as the side of the frustum of a superelliptical cone (Fig. 4C). The computational burden of the calculation of S_i using integration algorithms is prohibitive, so it is approximated by

$$S_i = S_{H_i}(P_i + P_{i+1})/2$$

where P_i and S_{H_i} are the perimeter and aver-

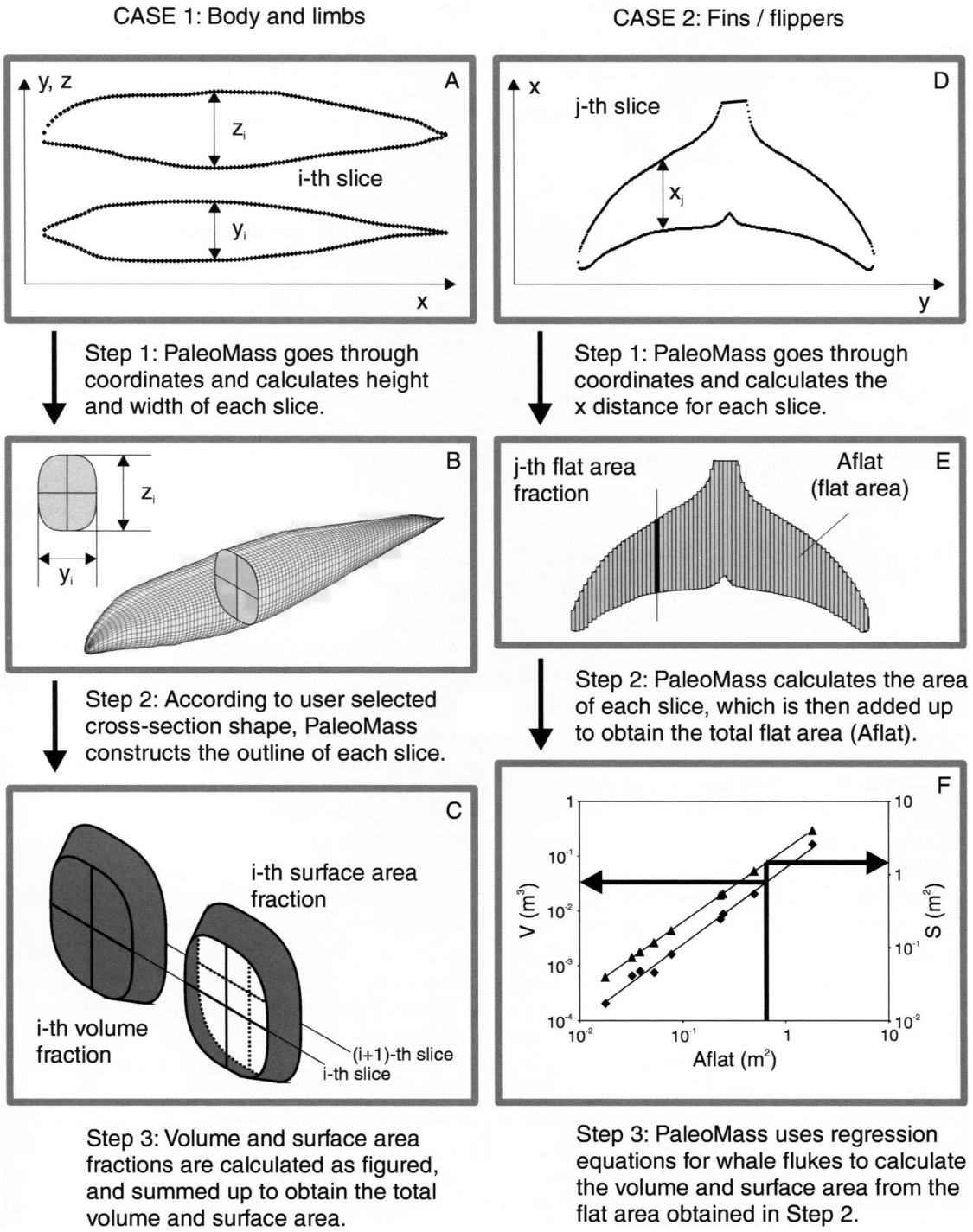

FIGURE 4. Outline of the computational process of the present method, as implemented in the computer program PaleoMass. Round structures, such as the body, and finlike structures are computed with different algorithms (left and right column, respectively).

TABLE 2. Results of least-square regressions on cetacean fluke measurements. The upper two rows are for complete flukes whereas the bottom two are for half the fluke, which are used for computation of asymmetrical finlike structures, such as dorsal fins and flippers. The standard allomatic equation $y = bx^a$ was used. See Table 1 for abbreviations.

Independent variable	Dependent variable	a	b	r^2
Aflat	S	0.998	2.22	1.00
Aflat	V	1.40	6.10E-02	0.993
Aflat/2	S/2	0.998	2.27	1.00
Aflat/2	V/2	1.40	8.04E-02	0.993

age slant height of the i^{th} cross-section, respectively. The perimeter of the superellipse, P_{SE}, is given as

$$P_{SE} = 4 \int_0^{0.5\pi} \{[2a \sin t(\cos t)^{(2-k)/k}]^2 + [2b \cos t(\sin t)^{(2-k/k)}]^2\}^{0.5}\, dt$$

The average slant height is calculated as

$$SH_i = \lambda_i \times SHright_i$$

where λ_i is the ratio of side areas between the right and oblique cone frustums and $SHright_i$ is the average slant height of the right cone frustum with the top and bottom surfaces identical to the ones in the i^{th} cone frustum. It should be noted that this heuristic method is not truly accurate, although it does provide sufficient accuracy as will be shown.

The volume and surface area of finlike structures are calculated from their flat areas (i.e., the areas of their two-dimensional images; Fig. 4D,E). Bose et al. (1990) examined the flukes of nine cetacean species and depicted the flat view and one cross-section for each of the flukes (Bose et al. 1990: Figs. 1, 2). Assuming that the cross-sectional shape is constant throughout a given fluke, I calculated its volume and surface area using these figures (Table 1). When plotting these calculated values against flat areas of the flukes, there is a high correlation (Table 2, Fig. 4F). Therefore, it is reasonable to use regression lines to estimate the volume and surface area of flukes from the flat areas (Fig. 4F). Constants obtained from least-square regression are given in Table 2. Caudal flukes are laterally symmetrical in flat view, but flippers and dorsal fin are not. Therefore, the regression equations for the flukes cannot be used for these latter structures. To facilitate approximation, I assumed that these structures behave like half a caudal fluke and calculated regression constants accordingly (Table 2).

Tests

I tested the method described above in three ways. I first used geometrical shapes of known volumes and surface areas to test the accuracy when the assumption of elliptical cross-section is met. The second test was done with commercial miniature models of extant animals, whose volumes are measurable. The third test was performed with actual aquatic vertebrates with known body masses, namely, two species of teleosts (*Scomber scombrus* and *Trachurus trachurus*) and Heaviside's dolphin (*Cephalorhynchus heavisidii*; [silhouettes based on Best 1988]).

Geometrical Shapes.—Using geometrical shapes, I tested the accuracy of the proposed method with changing major-axis angle and resolutions when the assumption of elliptical cross-sections is met. Henderson (1999) conducted a similar test for his method but only regarding the relationship between the accuracy of estimated volume and resolution. I used a prolate spheroid with a fineness ratio of 4.0, which approximates the values known for some living cetaceans (Massare 1988).

In the first subtest, I examined the tolerance of the method to changes in the angle of the major axis. The size of the spheroid was kept constant, with polar and equatorial radii of 1000 and 250 dots, respectively. The major semi-axis was initially set to the horizontal (0°), and then its angle was increased by 10° until 90° was reached (i.e., the major semi-axis was vertical). The result is given here in Figure 5A. The volume was constantly estimated with high accuracies between 99.1% and 99.5%, whereas the surface area was affected more substantially by changes in the angle of the major axis (accuracy varied between 98.0% and 103.7%). The number of slices was varied in the second subtest, which examined the tolerance of the method to resolution. The sampling rate of the major semi-axis was varied from 5 to 3000. The major semi-axis was kept

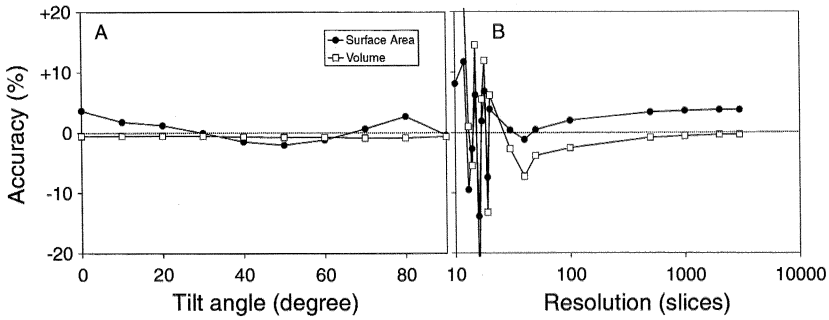

FIGURE 5. Results from the test of the present method using prolate spheroids. A, Test of axial angle, showing how the accuracy changes as the angle of the major axis increases from horizontal. B, Test of resolution, showing how the accuracy improves with increasing sampling rate (in number of slices). Note that the volume is almost always estimated with more than 99% of accuracy, regardless of the major-axis angle and as long as the slice count is high (about 1000 or more). The surface area estimates are less reliable.

horizontal in all cases. The accuracy of volume estimates asymptotically approaches 100% with increasing slice number, whereas the same for surface area estimates is about 104% (Fig. 5B). This error of about 4% seems to be common among calculations of perimeters and surface areas using computational integration: the perimeter estimation by ImageTool also shows a similar level of error.

Miniature Models.—Four commercially available models of vertebrates were used for this test (Table 3). The volumes of the models were measured in a one-liter measuring cylinder with 10-ml scales. The cylinder was first filled halfway (500 ml) with water, and then the model was submerged. Additional water was supplied from a syringe with 0.5-ml scales, until the water level reached the next graduated mark on the cylinder. The volume of the model was then calculated by subtracting the total volume of water (i.e., the original 500 ml plus the addition from the syringe) from the final reading of the cylinder. Two measurements per model were taken to obtain averages. No more than 1% difference was observed between the two measurements of each model. The lateral and dorsal view outlines of the models were obtained by scanning the models with a flatbed scanner. The scanned images were cropped in CorelPhotopaint 9 and converted to vector-based outlines in CorelTrace 9.

A horse model was treated differently from the others in that the body was separated into two pieces at the shoulder (Fig. 6). This is because the body axis bends at the shoulder. The present method is most accurate when the sampling axis is parallel to the body axis, so the neck and head were rotated as in Figure 6.

The models used are listed in Table 3, with the results of the tests. The volumes of the models were calculated with ranges ($2.0 < k < 2.5$), as discussed earlier. The volumes of the two terrestrial tetrapods (*Elephas* and *Equus*) fell within the calculated ranges, whereas one marine tetrapod (*Tursiops*) was bulkier than the higher end of the estimated range. The volume of the *Tursiops* model requires the average *k*-value of body cross-sections to be 3.3, which is far higher than 2.5. This discrepancy

TABLE 3. The results of the tests using miniature models of vertebrates.

Model	Estimated volume range (cc)	True volume (cc)	Equivalent *k*-value
Horse (*Equus*)	21–23	23	2.5
Asian elephant (*Elaphus*)*	130–137	135	2.3
Bottlenose dolphin (*Tursiops*)	163–174	186	3.3
Ichthyosaurus	75–80	91	4.1

* Without ears or tusks.

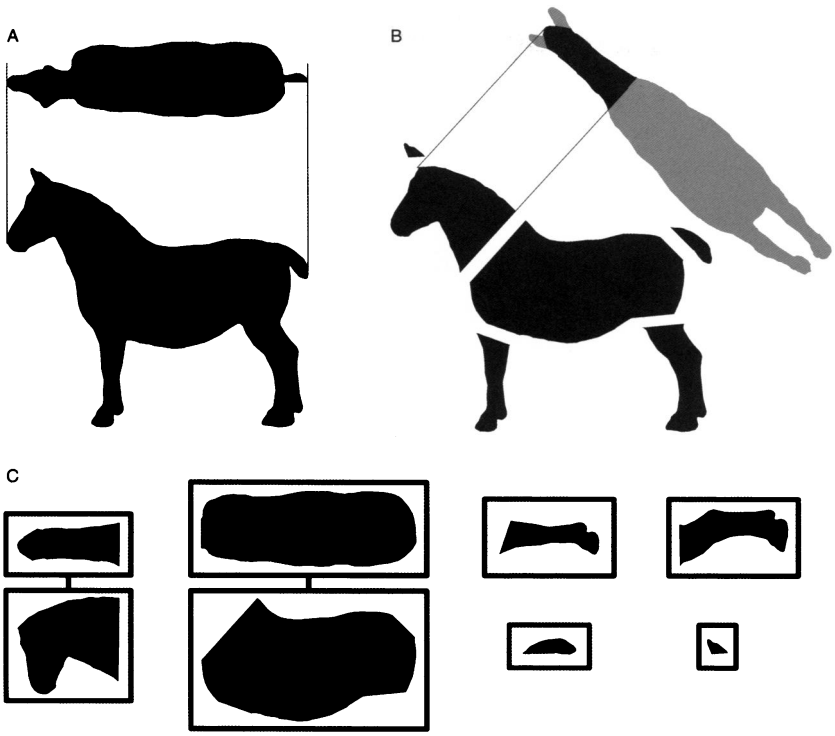

FIGURE 6. Division of horse silhouettes in practice. A, The lateral and dorsal views of a horse model. B, How the lateral view was divided into six, and posterodorsal view of the neck was added. C, The resulting eight images that were used in the analysis. The lines connecting two images indicate that the images are two orthogonal views of one structure.

will be discussed later. The model of *Ichthyosaurus* used is unusual in being almost triangular in body cross-sections. In three-dimensionally reconstructed specimens of *Stenopterygius* and *Ophthalmosaurus*, the body cross-sections are not triangular (e.g., Andrews 1915). These triangular cross-sections make the volume of the model much larger than elliptical cross-sections: it would require a *k*-value of 4.1 to approximate the volume with the superelliptical model.

Actual Animals.—The mass estimates of the three species examined are given in Table 4. The average density of the entire body was assumed to be that of seawater at 20°C (1024 kg/m^3 [Vogel 1994]). The superelliptical exponents were assumed to be $1.5 < k < 2.0$ for teleosts and $2.0 < k < 2.5$ for tetrapods, as discussed earlier. The body mass estimates for the three teleost individuals successfully approximated the true values, although a female *Trachurus* with eggs was marginally heavier than estimated (by 0.7%). For *Cephalorhynchus* the true body mass was much higher than the

TABLE 4. The results of the tests using actual animals. The true body masses of the two teleost species fell within the estimated ranges (0.7% error for one *Trachurus* with mature eggs), whereas Heaviside's dolphin was heavier than estimated.

Species	Estimated mass range (g)	True mass (g)	Equivalent *k*-value
*Scomber scombrus**	549–630	605	1.8
*Trachurus trachurus**	238–273	275	2.0
Trachurus trachurus	234–269	244	1.6
Cephalorhynchus heavisidii	48600–52100	56000	3.5

* Female with eggs.

estimated values: it requires the average *k*-value to be 3.5 to obtain the true body mass from calculation. Note that this value is similar to the one obtained for the model of another delphinid (*Tursiops*).

Discussion.—The results of the tests indicate the following: First, the volume estimation by the present method is reliable when the assumption of elliptical cross-sections is met, whereas the surface area is slightly overestimated (by 4%). Second, the method can be applied to actual animals, for which the assumption of elliptical cross-section is often not met, by giving ranges to estimated values. The range can be calculated by using empirical superelliptical exponents (*k*-values), which are $1.5 < k < 2.0$ for most teleosts and $2.0 < k < 2.5$ for most tetrapods.

Obvious exceptions to the above conclusions are cetaceans, which seem to have average *k*-values of above 3.0. No cross-sections of cetacean bodies were available for this study to confirm such high values. However, external observations suggest that they indeed have more rectangular body cross-sections than teleosts or terrestrial tetrapods. For example, an anterior view of a *Delphinapterus leucas* is approximated by a superellipse with a *k*-value of 3.0 when the flippers and dorsal fin are disregarded (Fig. 2I). The presence of high *k*-values in cetaceans can also be visually confirmed by comparing two three-dimensional models of *Cephalorhynchus* with *k*-values of 2.0 and 3.0, respectively (Fig. 7): the model with the *k*-value of 3.0 (Fig. 7A) seems more natural than the one with 2.0 (Fig. 7B). Also, the flippers are almost detached from the body when the *k*-value is assumed to be 2.0. Further support comes from Bose et al. (1990), who found the average error factor of 13.3% for the four cetaceans whose body mass was underestimated by the elliptical cross-section model they used. This average error factor equals having superelliptical cross-sections with a *k*-value of 3.11, which is comparable to the values obtained in this study. It should be noted, however, that the body mass was closely matched by the estimate (only 1.2% overestimation) for one of the cetaceans they examined (*Lagenorhynchus acutus*) (Bose et al. 1990).

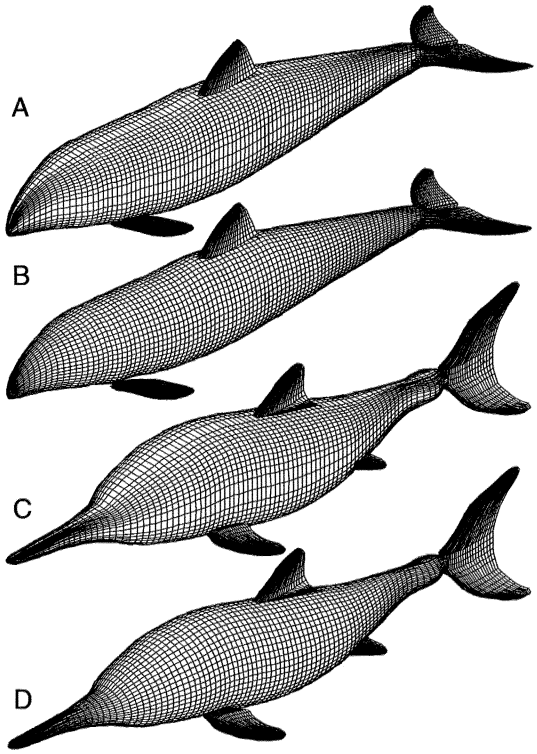

FIGURE 7. Three-dimensional models of two marine amniotes. A, *Cephalorhynchus heavisidii*, reconstructed with a constant superelliptical exponent (*k*-value) of 3.0 for body cross-sections. Based on orthogonal photographs provided in Best 1988. B, The same with *k*-value of 2.0 (i.e., elliptical cross-sections). C, *Stenopterygius quadriscissus* with *k*-value of 3.0. Based on PMU R158 and SMNS 54819. D, The same with *k*-value of 2.0.

Applications to Extinct Vertebrates

With the knowledge obtained from the above tests, I estimated the body mass and surface area for some extinct marine reptiles. The following assumptions were made: (1) the average *k*-value of body cross-sections is between 3.0 and 3.5, as in delphinid cetaceans examined in this study; (2) the average density of a given individual was that of seawater at 20°C (1024 kg/m^3 [Vogel 1994]). The average *k*-value of 4.1, obtained for a miniature model of *Ichthyosaurus*, is probably too high as discussed earlier, so it was not used for the present purpose. Two examples of three-dimensional reconstruction of the ichthyosaur *Stenopterygius* are given in Figure 7, to facilitate visual assessment of how the animal would look with two different *k*-values of 2.0 (i.e., elliptical cross-sections; Fig. 7D) and 3.0

TABLE 5. Body mass and surface area estimates for some Mesozoic marine reptiles. Institutional abbreviations: BSPM, Bayerische Staatssammlung für Paläontologie und historische Geologie, Munich; GPIT, Geologisch-Paläontologisches Institut, Tübingen; MHH, Museum Hauff, Holzmaden; PMU, Paleontologiska Museet, Uppsala Universitet; SMNS, Staatliches Museum für Naturkunde, Stuttgart.

Taxon	Specimen/ reference	L (m)*	Surface area (m^2)		Mass (kg)	
			k = 3.0	k = 3.5	k = 3.0	k = 3.5
Stenopterygius	SMNS 16811	2.40	2.64	2.69	163	168
	PMU R158	1.19	0.580	0.589	17.1	17.5
	Munich2	1.15	0.554	0.564	17.3	17.7
	TUB Re1297/1	1.11	0.447	0.456	13.3	13.7
	TUB Q07	1.06	0.444	0.451	11.7	12.1
	SMNS 56631	1.01	0.415	0.422	11.1	11.4
	Hauff9	0.957	0.382	0.389	9.10	9.34
	PMU R435	0.634	0.152	0.154	2.46	2.52
	SMNS 54818	0.598	0.144	0.146	2.26	2.32
	SMNS Small	0.450	0.0809	0.0823	0.900	0.924
Plesiosaurus	Hauff and Hauff 1981	2.94	2.66	2.71	172	177
Cryptoclidus	Brown 1981	4.0†	7.70	7.82	737	756
Rhomaleosaurus‡	Hauff and Hauff 1981	3.34	5.87	5.95	482	494
Platecarpus	Williston 1910	4.0†	3.72	3.79	246	253

* Fork length for *Stenopterygius*.
† Approximate value.
‡ Body based on dorsoventral view only.

(Fig. 7C). Both lateral and dorsal views were used whenever possible. It was necessary to combine the lateral view of one individual with the dorsoventral view of another with a similar body length to achieve this goal. In the case of *Stenopterygius*, the ventral view of SMNS 54819 was combined with the lateral views of ten specimens, after linearly adjusting the position of the pectoral and pelvic girdles of the former to the latter. This could compromise the accuracy of the outcome to some degree but is more reasonable than using only the lateral views, assuming that the width of the body cross-sections is equal to their height (e.g., Motani et al. 1999). The computations were made for ten ichthyosaurs, three plesiosaurs, and one mosasaur, and the results are given in Table 5.

The results obtained are untestable in a strict sense. However, it is possible to see how the results compare with the known body length-mass distribution of cetaceans. Body masses of twelve cetacean species collected from the literature (n = 198; see figure caption for details) are plotted against body lengths (fork length) in Figure 8A, with 95% prediction bands. Data for large whales are based on the studies by the Whales Research Institute, Tokyo, Japan, which indicate that some blood that escaped during the sawing process is not included in the body mass presented (see Introduction). However, *Physeter* and *Megaptera* seem to be on the same regression line as smaller cetaceans (Fig. 8A), suggesting that the amount of blood that escaped was not significant, as originally suspected by Nishiwaki and Hayashi (1950). *Balaenoptera* seems to be lighter than other whales of the same body length, forming its own distribution that is parallel to the distribution of the rest (dark gray in Fig. 8A).

When the estimated body masses of *Stenopterygius* were plotted against their fork lengths, the points fell near the midline of the cetacean distribution (Fig. 8B). This adds at least some confidence to the validity of the present method. For comparison, Figure 8C shows a plot of body mass approximations for the same genus, using a prolate spheroid model (Massare 1988). It is clear that the present method gives results that are more compatible with the cetacean data than the spheroid model does.

Discussion

There are advantages and a disadvantage to the present method, when compared to the one presented by Henderson (1999). The disadvantage lies in the inflexibility of the sampling axis: all slices of the present method are necessarily normal to the horizontal axis of the image (and thus the slices are parallel to

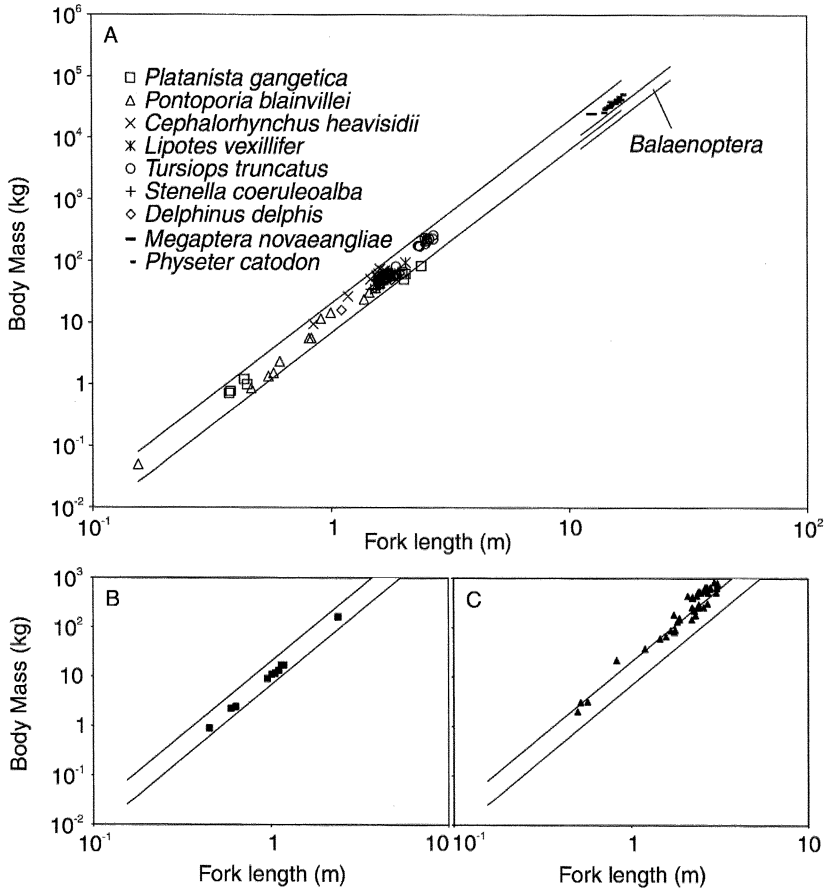

FIGURE 8. Body mass plotted against body length. A, Plot for 198 individuals of cetaceans: *Balaenoptera borealis* (n = 27; Fujino 1955); *B. musculus* (n = 34; Nishiwaki and Hayashi 1950; Nishiwaki and Oye 1951; Ohno and Fujino 1952); *B. physalus* (n = 34; Nishiwaki and Hayashi 1950; Nishiwaki and Oye 1951; Ohno and Fujino 1952); *Cephalorhynchus heavisidii* (n = 16; Best 1988); *Delphinus delphis* (n = 21; Gihr and Pilleri 1968); *Lipotes vexillifer* (n = 3; Gihr et al. 1979); *Megaptera novaeangliae* (n = 1; Ohno and Fujino 1952); *Physeter catodon* (n = 16; Ohno and Fujino 1952); *Platanista gangetica* (n = 9; Pilleri and Gihr 1976a); *Pontoporia blainvillei* (n = 14; Pilleri and Gihr 1976b); *Stenella coeruleoalba* (n = 12; Gihr and Pilleri 1968); *Tursiops truncatus* (n = 11; Fish 1993; Skrovan et al. 1999). Area in dark gray represents 95% prediction belt for *Balaenoptera*, whereas that in white is for the rest. B, Plot for *Stenopterygius* based on the present method, superimposed upon the prediction belt for non-*Balaenoptera* cetaceans. C, Plot for *Stenopterygius* based on the prolate spheroid model (Massare 1988).

each other), whereas Henderson's method allows its slices to be oblique to the horizontal axis. This characteristic may have effects when computing animals with bent body axes (such as the horse, whose neck is erect from the horizontal axis). However, there are indications that this factor does not cause significant shortcomings in the present method. First, the test using the horse model showed that the method is capable of giving reasonable estimates of its volume, as long as the inclined part of the body (i.e., neck in this case) was treated separately (Fig. 6C). Second, the test of major-axis angle showed that the present method is not affected by the inclination of the body axis, as long as the assumption of elliptical cross-sections is met. Third, many vertebrates, aquatic ones especially, have approximately straight body axes, which are suitable for the present method.

The first advantage of the present method is its high accuracy, as demonstrated earlier with three tests. This is achieved by the incorporation of the following factors: (1) high slice counts (or sampling rate) of over 1000; (2) absence of manual operation in obtaining coordinates from bitmap files of vertebrate silhouettes (raw data); and (3) superelliptical model

of body cross-sections. Henderson's (1999) method underestimated the volume of a simple ellipsoid by 1.2% with the slice count of 32 (Henderson 1999: Fig. 8). The value of 1.2% may appear to be sufficiently small, but it is not so, considering that this value is for a very simple case in which every assumption is met. Also, slicing an animal into 32 sections does not provide as accurate a reconstruction as doing the same to an ellipsoid. Animals have complicated outlines with multiple inflection points, and higher slice counts are necessary to achieve the same level of accuracy as for an ellipsoid. A table given by Henderson (1999: Table 3), comparing estimated and observed body masses, is not a rigorous test, because the estimation and observation values are based on different individuals, unlike in the present study. Also, the numbers are not as close as they may appear to be at first sight: a 3.6-m elephant was estimated to be 1.8% heavier than a 4.0-m individual (Henderson 1999: Table 3), whereas it should be about 27% lighter, if the body mass were to change according to the cube of the body length. The second advantage of the present method is in the use of range estimation, which increases the scientific value of the outcome. It is better to have a range of values based on an empirically tested method than a single value of unknown accuracy. The third advantage is the ease of computation, which only requires two free software packages and bitmap files as data.

Having an accurate calculation protocol may not seem important, given that most silhouettes are reconstructed subjectively by researchers and artists for extinct animals. However, accuracy in calculation still helps minimize the total error level. If the silhouette reconstruction had errors that are on the border of being acceptable (e.g., 5%), having inaccurate calculation would increase the error level to unacceptable values. The best we can do is to minimize the error at each stage of the body volume/surface area estimation, and therefore having accurate calculation protocol is important regardless of the accuracy of the silhouette to be used. Of course, it is important to reconstruct reasonable silhouettes, but it is beyond the scope of the present method, which is about the stage of estimation after having silhouettes. In some cases, approximate body outlines are preserved in fossils as in *Stenopterygius*, reducing the bias from silhouette reconstruction. The present method is effective in utilizing such rare information. Also, it is obviously desirable for neontological studies, where silhouettes can be obtained directly, to have an accurate calculation protocol.

It should be noted that the superelliptical model employed in the present method is not perfect: many cross-sections of vertebrate bodies are not superelliptical (Fig. 1). This, however, does not compromise the predictive value of the present method in volume-mass estimation. The present method makes estimates with ranges, so the exact match of the cross-sectional outline is not very important, as long as the actual cross-sectional area lies between those of the two superellipses that define the upper and lower limits. Surface area estimation is more problematic than volume-mass estimation. Actual perimeters are usually much larger than superelliptical perimeters. Ignoring this factor, as in Henderson (1999) and the present study, should lead to some degree of underestimation of the true surface area. This underestimation (up to 23% in some cases, judging from Figure 1) is partly compensated for by the slight tendency to overestimate surface area, typical of the algorithms used in the present method (about 4%). Still, the overall tendency is probably to underestimate surface area, on average.

The present method can be modified to incorporate center of mass estimation. Doing so, however, would require the distribution pattern of *k*-values along the body axis, as well as differential density distribution within the body, to be known. It is generally true that the anterior part of the body tends to have *k*-values higher than 2.0, whereas the values are often 2.0 or less in the posterior part of the body (especially in the tail). This suggests that assuming a constant *k*-value for the entire body, as in Henderson's (1999) study and this one, would produce a bias toward posterior displacement of the estimated center of mass from the true position. It would require extensive research of extant animals to establish a

common pattern of *k*-value distribution, which is beyond the scope of the present study. Estimation of the center of mass in extinct animals is not yet as reliable as desired.

Conclusions

Body mass estimates based on orthogonal silhouettes of vertebrates necessarily incorporate errors. The largest and most generally acknowledged source of error is the assumption that the ellipse can approximate the cross-sections of vertebrate bodies. The superellipse, which occurs in nature and encompasses ellipses, can be used to improve the accuracy of cross-sectional modeling, and hence of body mass estimation. A computerized method to estimate body masses is given, and a new computer program that performs this task (PaleoMass) is introduced. The method incorporates superelliptical cross-sections and high density slicing to achieve high accuracies. Testing of the method, using geometrical shapes, miniature vertebrate models, and actual animals, supports the validity of the model in practice. The method is also applicable to extinct animals by giving estimates with ranges. The method can be improved in the future by increasing the quality and quantity of empirical data on vertebrate body cross-sections.

Acknowledgments

I thank C. McGowan for his continuous supports to my projects. F. Fish, D. Henderson, C. McGowan, K. Padian, P. L. Rosin, and H.-D. Sues provided useful suggestions on earlier versions of the manuscript. This study was supported by a Natural Sciences and Engineering Research Council grant (A9950) to C. McGowan.

PaleoMass program is available from PaleoNet website (http://www.nhm.ac.uk/hosted_sites/paleonet/).

Literature Cited

Alexander, R. M. 1985. Mechanics of posture and gait of some large dinosaurs. Zoological Journal of the Linnean Society 83: 1–25.

———. 1998. All-time giants: the largest animals and their problems. Palaeontology 41:1231–1245.

Andrews, C. W. 1915. Note on a mounted skeleton of *Ophthalmosaurus icenicus* Seeley. Geological Magazine, new series, 6: 145–146.

Barr, A. H. 1981. Superquadrics and angle-preserving transformations. IEEE Computer Graphics and Applications 1:11–23.

Best, P. B. 1988. The external appearance of Heaviside's dolphin, *Cephalorhynchus heavisidii* (Gray, 1828). Report of International Whaling Commission, Special Issue 9:279–299.

Bose, N., and J. Lien. 1989. Propulsion of a fin whale (*Balaenoptera physalus*): why the fin whale is a fast swimmer. Proceedings of the Royal Society of London B 237:175–200.

Bose, N., J. Lien, and J. Ahia. 1990. Measurements of the bodies and flukes of several cetacean species. Proceedings of the Royal Society of London B 242:163–173.

Brown, D. S. 1981. The English Upper Jurassic Plesiosauroidea (Reptilia) and a review of the phylogeny and classification of the Plesiosauria. Bulletin of the British Museum (Natural History), Geology 35:253–347.

Bryant, H. N., and A. P. Russell. 1992. The role of phylogenetic analysis in the inference of unpreserved attributes of extinct taxa. Philosophical Transactions of the Royal Society of London B 337:405–418.

Colbert, E. C. 1962. The weights of dinosaurs. American Museum Novitates 2076:1–16.

Cong, L., L. Hou, X. Wu, and J. Hou. 1998. The gross anatomy of *Alligator sinensis* Fauvel. Science Press, Beijing. [In Chinese.]

Dewar, H., J. B. Graham, and R. Brill. 1994. Studies of tropical tuna swimming performance in a large water tunnel. II. Thermoregulation. Journal of Experimental Biology 192:33–44.

Fish, F. E. 1993. Power output and propulsive efficiency of swimming bottlenose dolphins (*Tursiops truncatus*). Journal of Experimental Biology 185:179–193.

———. 1998. Comparative kinematics and hydrodynamics of odontocete cetaceans: morphological and ecological correlates with swimming performance. Journal of Experimental Biology 201:2867–2877.

Fujino, K. 1955. On the body weight of the Sei Whales located in the Adjacent Waters of Japan (II). Scientific Reports of the Whales Research Institute, Tokyo, Japan 10:133–141.

Gardner, M. 1965. The "superellipse": a curve that lies between the ellipse and the rectangle. Scientific American 1965(21): 222–236.

Gihr, M., and G. Pilleri. 1968. On the anatomy and biometry of *Stenella styx* Gray and *Delphinus delphis* L. (Cetacea, Delphinidae) of the Western Mediterranean. Investigations of Cetacea 1:15–65.

Gihr, M., G. Pilleri, and K. Zhou. 1979. Cephalization of the Chinese River Dolphin *Lipotes vexillifer* (Platanistoidea, Lipotidae). Investigations of Cetacea 10:257–274.

Gilbert, S. G. 1968. Pictorial anatomy of the cat. University of Washington Press, Seattle.

Graigie, E. Horne. 1966. A laboratory guide to the anatomy of the rabbit, 2d ed. University of Toronto Press, Toronto.

Gregory, W. K. 1905. The weight of the *Brontosaurus*. Science, new series, 22(566):572.

Hauff, B., and R. B. Hauff. 1981. Das Holzmadenbuch. Repro-Druck GmbH, Fellbach.

Henderson, D. M. 1999. Estimating the masses and centers of mass of extinct animals by 3-D mathematical slicing. Paleobiology 25:88–106.

Massare, J. A. 1988. Swimming capabilities of Mesozoic marine reptiles: implications for method of predation. Paleobiology 14:187–205.

Mori, O., T. Ogawa, H. Ouchi, and T. Mori. 1982. Anatomy 1. Kimbara Press, Tokyo. [In Japanese.]

Motani, R., B. M. Rothschild, and W. Wahl Jr. 1999. Large eyeballs in diving ichthyosaurs. Nature 402:747.

Murayama, T., and F. Kasamatsu. 1996. Kokomade wakatta iruka to kujira. [We know this much about whales and dolphins.] Kodansha Bluebacks, Tokyo. [In Japanese.]

Nishiwaki, M., and K. Hayashi. 1950. Biological investigation of

Fin and Blue Whales taken in the Antarctic season 1947–48 by the Japanese fleet. Scientific Reports of the Whales Research Institute, Tokyo, Japan 3:132–190.

Nishiwaki, M., and T. Oye. 1951. Biological investigation of Blue Whales (*Balaenoptera musculus*) and Fin Whales (*Balaenoptera physalus*) caught by the Japanese Antarctic whaling fleets. Scientific Reports of the Whales Research Institute, Tokyo, Japan 5:91–167.

Ohno, M., and K. Fujino. 1952. Biological investigation on the whales caught by the Japanese Antarctic whaling fleets, season 1950/1951. Scientific Reports of the Whales Research Institute, Tokyo, Japan 7:125–188.

Pilleri, G., and M. Gihr. 1976a. On the embryology of *Platanista gangetica*. Investigations of Cetacea 7:45–64.

———. 1976b. On the embryology of the La Plata Dolphin *Pontoporia blainvillei*. Investigations of Cetacea 7:65–89.

Pilu, M., and R. B. Fisher. 1995. Equal-distance sampling of superellipse models. Proceedings of the British Machine Vision Conference 1:257–266.

Rosin, P. L., and G. A. W. West. 1995. Curve segmentation and representation by superellipses. IEEE Proceedings on Visual Image Signal Process 142:280–288.

Schmidt-Nielsen, K. 1997. Animal physiology: adaptation and environment, 5th ed. Cambridge University Press, Cambridge.

Skrovan, R. C., T. M. Williams, P. S. Berry, P. W. Moore, and R. W. Davis. 1999. The diving physiology of bottlenose dolphins (*Tursiops truncatus*). II. Biomechanics and changes in buoyancy at depth. Journal of Experimental Biology 202:2749–2761.

Vogel, S. 1994. Life in moving fluids: the physical biology of flow, 2d ed. Princeton University Press, Princeton, N.J.

Walker, W. F., and D. G. Homberger. 1992. Vertebrate dissection, 8th ed. Saunders College Publishing, Forth Worth, Tex.

Williston, S. W. 1910. A mounted skeleton of *Platecarpus*. Journal of Geology 18:537–541.

Witmer, L. M. 1995. The extant phylogenetic bracket and the importance of reconstructing soft tissues in fossils. Pp. 19–33 *in* J. J. Thomason, ed. Functional morphology in vertebrae paleontology. Cambridge University Press, Cambridge.